VEGETATION CLASSIFICATION USING SEASONAL VARIATIONS AT C- AND Ku-BAND

Gardner Watt, Perry Hardin, and David G. Long
Brigham Young University, MERS Laboratory
459 CB, Provo, UT 84602
801-378-4383, FAX: 801-378-6586 long@ee.byu.edu

Abstract–Using C-band data (h-pol) from the ERS-2 AMI scatterometer and Ku-band data (dual-pol) from the NASA Scatterometer we study the seasonal signatures of key vegetation classes in North America. We compare the seasonal responses of vegetation types defined by both Matthew's classification and the University of Maryland AVHRR-based classification. We then use the seasonal response in a series of vegetation classification experiments.

INTRODUCTION

σ_o has been shown to be sensitive to changes in ice and land in regional studies over the Boreal forest regions in Canada, and over the Siberian Forests [1]. During the summer, the variation in the backscatter coefficient over these land areas is dependent usually on soil and vegetation moisture while during the winter, soil freezing and snow cover drastically change the response of σ^o. Scatterometers have also been used in tropical vegetation studies [2]. Since scatterometers are capable of global coverage and can map the entire world over a few days in all weather conditions, regional vegetation classification by scatterometers is potentially very useful. In this paper we study the seasonal response of the radar backscatter from various vegetation types and use it to classify vegetation.

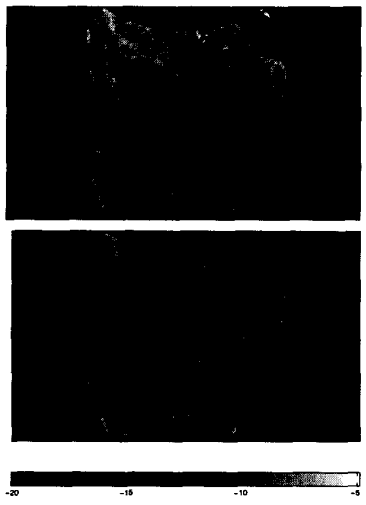

Figure 1: SIR $\mathcal{A}$ images over North America for NSCAT-V (upper) and ERS-2 (lower).

Data from the European Remote Sensing (ERS-1/2) AMI instruments (Scatterometer mode) and NASA's Scatterometer (NSCAT) are used in this study. The ERS-1/2 scatterometers are single polarization (vertical) and operate in the C-band at 5.3 GHz. NSCAT was a dual-polarization (vertical and horizontal) scatterometer that operated at 14 GHz in the Ku-band from October 1996 to July of 1997. These instruments are used in this study in order to look at the seasonal response of vegetation at two different bands.

A linear scattering model is used to relate σ^o (dB) with incidence angle for incidence angles from $22° - 55°$,

$$\log \sigma^o = \mathcal{A} + \mathcal{B}(\theta - 40°) \quad (1)$$

where $\mathcal{A}$ is σ^o at 40° incidence angle and $\mathcal{B}$ is the incidence angle dependence of σ^o. In this study the $\mathcal{A}$ and $\mathcal{B}$ values are estimated using the SIR resolution enhancement algorithm [2]. Fourteen days of data over North America are used in this analysis. Sample $\mathcal{A}$ images are given in Fig.1.

σ^O VARIATION OVER VEGETATION REGIONS

To study the backscatter over different vegetation classes, eight vegetation types from North America were chosen using two vegetation maps: the Matthews Global Vegetation, Land Use, and Seasonal Albedo data set from the National Oceanic and Atmospheric Administration (NOAA) and the University of Maryland vegetation map [4] derived from AVHRR data. A selection of compatible vegetation classes was created that combines the different vegetation descriptions of each data set to aid in the comparison. Combining the categories of the two maps was not a trivial matter since the Matthews vegetation map has over 30 separate categories for the vegetation described throughout the world, while the AVHRR derived map has twelve vegetation categories. In combining the two maps care was taken to preserve similar vegetation descriptions. Table 1 lists the selected vegetation classes as well as their percentage of coverage over North America. Figure 2 shows the corresponding vegetation maps.

For each vegetation class, an average value of σ^o was calculated from the corresponding pixels of each 14-day $\mathcal{A}$ image and plotted versus time (Figs. 3 and 4). No separation by latitude was attempted in this initial study. For each class a different seasonal response signature is apparent. It is also clear that the seasonal re-

0-7803-5207-6/99/$10.00 © 1999 IEEE.

Table 1: Vegetation classes and pixel percentages over North America

Veg Class	Vegetation type	Matthews	AVHRR
1	Evergreen needleleaved forests	29.8	28.4
2	Deciduous forests with evergreens/mixed forests	17.7	14.8
3	Deciduous forests	10.3	4.9
4	Xeromorphic shrublands/shrubland/closed bushlands	9	2
5	Grassland with shrub cover/open shrublands	5.6	8.1
6	Woodlands/grasslands with woody cover	5.3	9.1
7	Tall, medium, short grasslands, meadows/croplands	19	31.3
8	Arctic alpine tundra, mossy bog/mosses and lichens	3.2	1.4

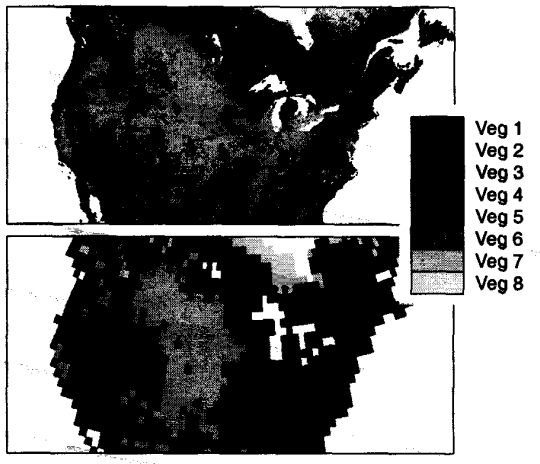

Figure 2: Selected vegetation classes for Matthews and AVHRR maps over North America.

sponses differ between C-band and Ku-band. The variations in the seasonal response are the motivating factors in using this data for vegetation classification.

METHODOLOGY

Using singular value decomposition (SVD), the seasonal response of each vegetation class is used to train a quadratic classifier. We first let $X = [X_1|X_2|...X_N]$ where N is the

Figure 3: Average Ku-band $\mathcal{A}$ seasonal response.

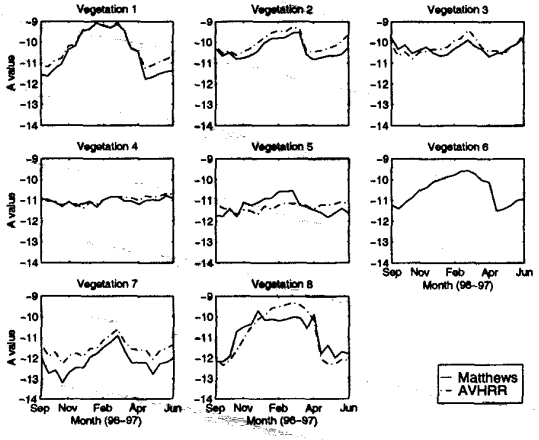

Figure 4: Average C-band $\mathcal{A}$ seasonal response.

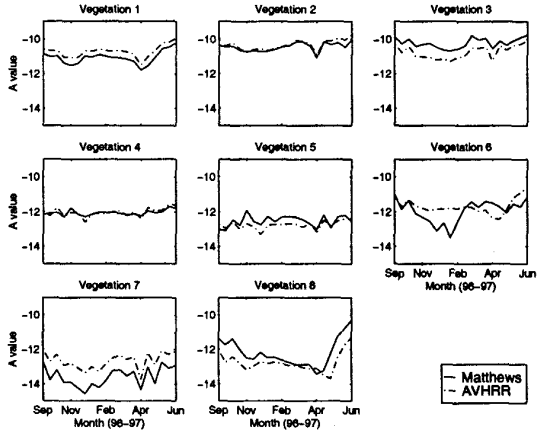

number of vegetation regions and $X_1, X_2, ..., X_N$ are vectors of σ^o at each seasonal sample, i.e. the seasonal response of each vegetation class. The SVD of X is then $X = U\Gamma V$, The columns of U are a basis set containing the most prominent seasonal responses (i.e., the principal component responses) of each vegetation region. X is expressed as a linear combination of the columns of U or, $X = \sum_i a_i U$. These a_i's are used as the classification centroids.

The seasonal response of each pixel in the image is projected onto the basis set, $r_i = U^{\dagger} x_i$, where x_i is the seasonal response of the i_{th} pixel. The vegetation class of a given pixel is classified using:

$$Im(i) = \min_j [(r_i - a_j)' R_j^{-1} (r_i - a_j) + \log |R_j|] \qquad (2)$$

where R_j is the sample covariance of the projection of the seasonal response of each vegetation region, r_i is the pixel response and a_j is the centroid of each vegetation region. Here Im is the final classified vegetation map. The above expression is a form of a Maximum-likelihood classifier.

RESULTS

Using this method, a number of classified vegetation maps were created based on the initial use of the Matthews and AVHRR-based vegetation maps for both ERS-2 $\mathcal{A}$ images and NSCAT-V images. The resulting classification images

Table 2: Confusion matrices for vegetation classification using NSCAT and ERS-2 data.

Matthews	NSCAT-V								ERS-2							
Regions	Veg 1	Veg 2	Veg 3	Veg 4	Veg 5	Veg 6	Veg 7	Veg 8	Veg 1	Veg 2	Veg 3	Veg 4	Veg 5	Veg 6	Veg 7	Veg 8
1	43.6	5.6	4.1	8.1	10.4	10.5	4.3	10.6	23.3	6.1	7.7	18.3	4.8	2.0	1.8	33.2
2	2.2	52.6	22	10.4	0.8	2.7	4.9	0.4	5.0	29.3	34.0	18.1	1.7	2.9	2.7	2.4
3	0.6	7.8	80.0	4.7	0.3	0.4	4.2	0.0	0.5	5.3	74.8	9.3	1	6	1.0	0.1
4	0.7	3.1	4.4	77.5	9.8	0.6	2.4	0.3	1.7	0.5	1.7	78.5	13.3	0.5	2.4	0.3
5	3.2	2.9	1.9	41.0	40.4	1.2	8.8	0.3	3.9	0.3	1.6	31.8	54.7	0.4	6.6	0.3
6	1.4	7.6	44.5	7.3	6.9	7.9	24.1	0.1	0.2	1.7	19.7	1.9	4.8	64.8	6.2	0.6
7	2.4	0.8	4.3	12	13.9	3	63.3	0.4	1.9	0.4	2.4	7.5	14.1	12.8	60.2	0.7
8	26.5	0.5	0.7	0.4	2	14.7	1.0	50.6	7.6	0.1	3.4	3	0.7	1.9	1.1	78.6

AVHRR	NSCAT-V								ERS-2							
Regions	Veg 1	Veg 2	Veg 3	Veg 4	Veg 5	Veg 6	Veg 7	Veg 8	Veg 1	Veg 2	Veg 3	Veg 4	Veg 5	Veg 6	Veg 7	Veg 8
1	39.9	20	4.5	12.8	1.2	10.6	3.2	6.3	35.6	8.7	3.9	32.1	3.3	7.2	1.9	5.9
2	7.2	69.2	7.3	10.0	0.6	1.3	2.8	0.5	12.7	40.7	7.4	29.8	3.2	1	3.1	1.0
3	6.2	39.2	31.5	8.4	0.8	2.2	9	2.1	10.3	21.8	25.6	28.5	3.3	1.6	7.4	0.8
4	0.6	2.1	0.3	71.4	15.3	1.3	6.8	0.4	0.7	0.6	0.8	65.7	20.3	2.2	7	0.8
5	0.5	1.6	0.5	55.5	27.6	1.4	11.7	0.7	0.2	0.9	0.6	48.7	34.9	2.2	10.6	1.5
6	10.8	6	1.1	15.2	2.4	42.8	2.1	18.5	11.7	2.9	2.2	26.5	8.4	23.6	4.9	18.7
7	2.9	10.0	13.1	14.5	8.5	2.0	46.9	1.5	3.3	3.8	14.1	15.3	15.3	5.4	39.7	2.4
8	0.70	0.1	0.4	0.3	0.4	9.7	2.8	74.9	3.6	1	1.7	2.5	3.6	7.5	2.5	66.6

can be seen in Fig. 5. To quantitatively compare the classification schemes, accuracy and inaccuracy assessments are done on the classifications using the accuracy assesment scheme in [3] which is derived from the Kullback-Leibler information metric. The usual class-averaged and overall accuracies are also given in Table 3.

Figure 5: Vegetation Classification over North America using the AVHRR derived vegetation map (top images) and the Matthews vegetation map (bottom images). The left images show the classifications using the NSCAT-V $\mathcal{A}$ image. The right images are based on the ERS-2 $\mathcal{A}$ image.

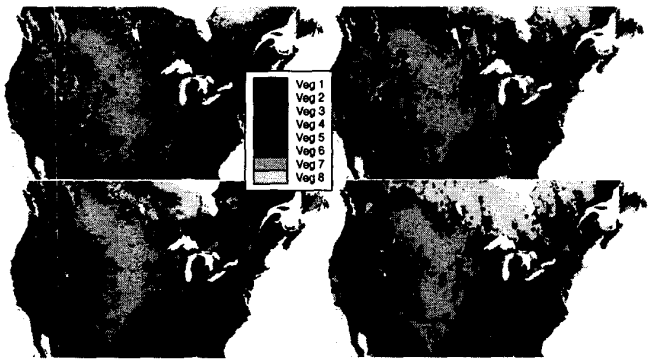

Table 3: Class-average, overall accuracy, and J_p coefficients for the classification analysis

		C(X)	A(X)	$J_p(X)$
NSCAT	Matthews	.5301	.5455	.5036
	AVHRR	.5212	.4694	.4535
ERS-2	Matthews	.5897	.4768	.4245
	AVHRR	.4296	.3706	.3623

CONCLUSIONS

There is a significant difference in the seasonal response of σ^o of the various vegetation classes. Using this fact we can classify different vegetation regions using singular value decomposition and a maximum likelihood classifier with a moderate degree of accuracy. Considering the limitations of the reference vegetation maps, the classifications exhibit a high degree of accuracy and consistency. The primary confusion observed is between related vegetation classes of similar canopy density. We believe that coupling scatterometer data with AVHRR data could improve the accuracy of global vegetation maps.

REFERENCES

[1] J. Pulliainen, N. Walkder, T. Manninen, M. Hallikainen and J. Grandell, "Land Applications of ERS-1 Wind Scatterometer in Boreal Forest Zone," *Proceedings of the International Geoscience and Remote Sensing Symposium*, pp. 1826-1828, Singapore, 4-8 August, 1997.

[2] D.G. Long and P. Hardin, "Vegetation Studies of the Amazon Basin Using Enhanced Resolution Seasat Scatterometer Data," *IEEE Transactions on Geoscience and Remote Sensing*, Vol. 32, No. 2, pp. 449-460, Mar. 1994.

[3] R. Nishii, S. Tanaka, "Accuracy and Inaccuracy Assessments in Land-Cover Classification," *IEEE Transactions on Geoscience and Remote Sensing*, Vol. 37, No. 1, pp. 491-497, Jan. 1999.

[4] "Global Land Cover mapping using AVHRR data," http://www.geog.umd.edu/landcover/lc/projects.html